Observation of dd excitations in NiO and NiCl$_2$ using K-edge resonant inelastic x-ray scattering

Michel van Veenendaal,[1,2] Xiaosong Liu,[3] Matthew H. Carpenter,[4] and Stephen P. Cramer[3,4]

[1]*Department of Physics, Northern Illinois University, De Kalb, Illinois 60115, USA*

[2]*Advanced Photon Source, Argonne National Laboratory, 9700 South Cass Avenue, Argonne, Illinois 60439, USA*

[3]*Physical Biosciences Division, Lawrence Berkeley National Laboratory, 1 Cyclotron Road, Berkeley, California 94720, USA*

[4]*Department of Applied Science, University of California, Davis, California 95616, USA*

The presence of dd excitations in K-edge resonant inelastic x-ray scattering in the $1s \rightarrow 4p$ region of transition-metal compounds and their excitation mechanism is established through measurements of NiO and NiCl$_2$. It is demonstrated that the valence excitations are due to the interaction between the excited $4p$ electron and the $3d$ valence electrons. A detailed analytical framework for interpreting these excitations in transition-metal compounds is presented, demonstrating a strong angular dependence for different dd excitations.

I. INTRODUCTION

The study of complex materials under real conditions is often hampered by the lack of proper characterization tools that are both chemical and bulk selective. In optical spectroscopy, one is unable to distinguish excitations from different elements and, for transition-metal compounds, dd excitations are only allowed due to the simultaneous excitation of magnons or phonons. Resonant inelastic x-ray scattering (RIXS),[1] on the other hand, employs the excitation of an electron from a deep-lying core level of a particular element into the valence shell through the absorption of an x-ray photon with energy $\hbar\omega$. One subsequently detects the energy $\hbar\omega'$ of the x rays resulting from the radiative decay of the core hole. Local dd transitions,[1] spin-flips,[2] and single-magnon excitations[3] have been observed in the soft x-ray region at the transition-metal L and M edges. However, low-energy x rays do not have sufficient penetration depth to study, for example, the electronic structure in technologically relevant materials, such as transition-metal molecular compounds in solution. The use of hard x rays allows the chemically selective measurement of valence excitations under ambient conditions. For example, for nickel compounds, the focus of this paper, Ni is at the active site of several environmentally critical enzymes.[4] These include enzymes for H$_2$ production [(NiFe) hydrogenase],[5] CH$_4$ production (methyl-coenzyme M reductase),[6] and CO-CO$_2$ metabolism (CO dehydrogenase).[7] Given the multitude of controversies about the catalytic mechanisms of these enzymes, a new experimental probe of the electronic structure of nickel and other transition-metal compounds would have immediate application in this field.

At the K edge, in the dipolar $1s \rightarrow 4p$ region, the focus of RIXS has been primarily on charge-transfer excitations with an energy of 2–6 eV.[8] These are generally considered to be a result of shakeup processes due to the strong Coulomb interaction with the $1s$ core hole. Low-energy excitations (< 2 eV) in the hard x-ray region are more difficult to observe, but will become more easily accessible due to the rapidly increasing advances in RIXS technology.[9–11] It has been shown that the $1s$ core-hole potential can possibly create bimagnon excitations.[10] In the weak preedge feature, which is due to $1s \rightarrow 3d$ transitions, dd excitations can be observed since angular momentum is transferred via the polarization of the x rays.[9] However, they are not expected at the main edge ($1s \rightarrow 4p$ transitions), since the $1s$ core-hole potential cannot transfer angular momentum to the valence shell. Despite that, low-energy excitations are still observed at these absorption energies.[11] In the absence of a clear understanding of the excitation mechanism, a definite assignment of low-energy excitations in the dipolar region ($1s \rightarrow 4p$) remains difficult.[10,11]

We demonstrate the presence of low-energy excitations in NiO and NiCl$_2$ in the $1s \rightarrow 4p$ excitation region. Since these materials are well studied, we can unequivocally ascribe the excitations to local dd transitions. We show that these excitations are a result of the $3d$-$4p$ Coulomb interaction. This mechanism leads to a clear angular dependence, which allows distinction from other low-energy excitations, such as, for example, bimagnons.[10] This work opens the door to the study of active sites using hard x rays.

II. EXPERIMENT

The experiments were performed at the MERIX undulator beamline of Sector 30 at the Advanced Photon Source, National Laboratory. Two monochromators are installed on the beamline. The first one is a water-cooled two-crystal diamond [111] monochromator with a measured bandwidth of 400 meV near the Ni K edge. The second one is a four-crystal backscatter monochromator with 70-meV resolution. The surface of the sample is aligned along $45°$ from the direction of beam incidence. The scattering angle is $90°$. The fluorescence emission is detected with a near-backscatter spherically bent diced-crystal spectrometer. The crystal analyzer has a 1-m radius of curvature and 1-mm^2 segments (pixels), and is immersed in a He atmosphere chamber to minimize scattering and absorption. A position-sensitive Si strip detector with 50-μm strips records the dispersed x rays from the analyzer. The sample-analyzer-detector geometry is arranged on a Rowland circle, with the sample and analyzer in fixed positions and the detector movable about the circle. Two crystal analyzers were used: [642] Ge (resolution of 180 meV) and [01-10] LiNbO$_3$ (resolution of 140 meV) for energies above 8.342 keV.

The RIXS spectra are shown in Fig. 1 at different excitation energies for a single-crystal NiO[001] and polycrystalline NiCl$_2$. In the preedge region, quadrupolar transitions from
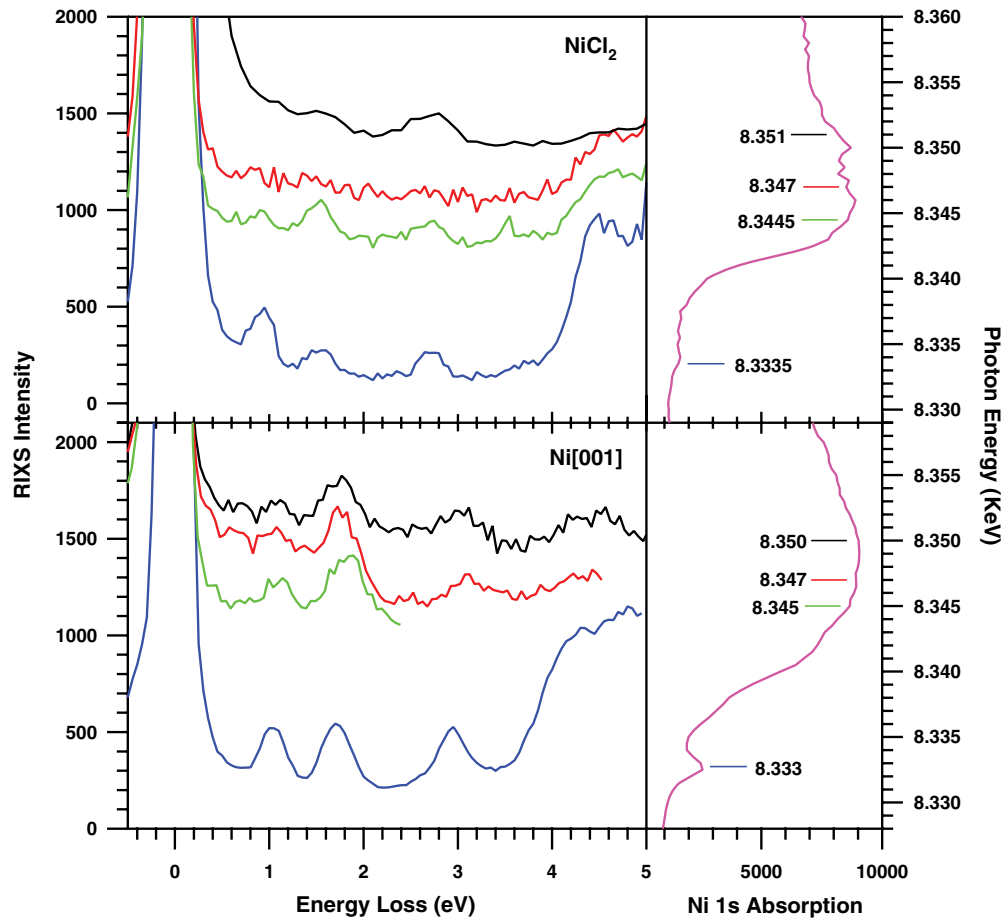
FIG. 1. (Color online) Ni K-edge RIXS of NiO[001] and NiCl$_2$. The x-ray absorption is shown in the right panel. RIXS spectra for different excitation energy are shown in the left panel.

the $1s$ into the $3d$ shell are observed. The dd transitions can be explained within an atomic multiplet framework.[9] In octahedral symmetry,[12] the ground state for Ni^{2+} is $\underline{d}^2_{e_g\uparrow}$ ($^3A_2$), where $\underline{d}_{e_g}$ stands for a $3d$ hole of e_g symmetry. The scattering causes $\underline{d}^2_{e_g} \rightarrow \underline{d}_{e_g}\underline{d}_{t_{2g}}$ transitions. In the absence of $1s$ spin-orbit coupling, spin is conserved. The final states that can be reached are of $^3T_1$ and $^3T_2$ symmetry. The $^3T_2$ is at 1 eV. The $\underline{d}_{e_g}\underline{d}_{t_{2g}}$ ($^3T_1$) configuration couples via the d-d Coulomb interaction to the $\underline{d}^2_{t_{2g}}$ state of the same symmetry and leads to peaks at 1.7 and 3 eV. A weak feature might also be visible around 0.5 eV, although it is hard to distinguish at this count rate due to the close proximity to the elastic line.

When increasing the excitation energy above the preedge feature, these local dd transitions are still visible. This is unexpected since quadrupolar features are very weak in the main absorption feature. Recently, dd features have also been observed in the $1s \rightarrow 4p$ region[11] in the quasi-zero-dimensional compound CuB$_2$O$_4$. Surprisingly, the strength in the preedge region of these excitations is rather small. Generally, excitations at the K edge are shakeup excitations resulting from the transient presence of a strong core-hole potential in the intermediate state.[8,13,14] However, since the ground state contains only e_g holes, the involvement of t_{2g} electrons in the screening process is unlikely. In addition, the

experiments are performed in a 90° scattering condition. This eliminates the possibility that the transitions are a result of the $\mathbf{A}^2$ term,[15,16] which is zero in this geometry. Also, since the polarization vectors of the incoming and outgoing x rays are perpendicular to each other, the orbital of the excited electron must have changed and the $4p$ electron can most likely not be considered a spectator. This change could be a result of hybridization between the $3d$ and $4p$ states on the site with the $1s$ core hole. This coupling is weak, and for a quasi-zero-dimensional compound, such as CuB$_2$O$_4$, it is symmetry forbidden.[11] The coupling is present in three-dimensional systems, such as NiO and NiCl$_2$. However, it is difficult to understand why a hybridization mechanism would favor one particular $t_{2g}e_g$ multiplet over another. One would expect that a hybridization mechanism would give equal weight to the $^3T_2$ peak and the combined $^3T_1$ features. This is confirmed via numerical calculations based on a tight-binding model to estimate the $3d$-$4p$ mixing throughout the Brillouin zone (not shown). However, this contradicts with the experimental observations where the $^3T_2$ is significantly weaker (see Fig. 1). Here, we demonstrate that the dd features are due to Coulomb scattering of the excited $4p$ electron with the $3d$ states.

The relative strength of these excitations compared to the charge-transfer features at 4 eV and higher might at first seem surprising since the $3d$-$4p$ Coulomb interaction is significantly

weaker than the $1s$-$3d$ interaction. In addition, the intensity of the transitions is approximately proportional to the square of the interaction strength. Charge-transfer excitations are excited by the interaction between the core-hole and valence shell, which is of the order of 6–8 eV. The dd excitations are due to higher-order terms in the $3d$-$4p$ Coulomb interaction, which are of the order of tenths of an electron volt. This makes the excitation process about a factor of 1000 smaller. Indeed, these transitions are not visible in most scattering geometries. However, experimentally, a (typical) $90°$ horizontal-scattering condition is employed, which very strongly reduces the charge-transfer excitations since the incoming polarization vector is perpendicular to both outgoing polarization vectors. For a single NiO_6 cluster, the charge-transfer excitations are then forbidden. Within a crystal, these transitions become weakly allowed away from high-symmetry directions in the Brillouin zone. In addition, the resonant factor reduces the intensity by a factor of $1/(E_f - E_g)^2$, where $E_f - E_g$ is the energy loss of the photon. This reduces the charge-transfer excitations by a factor of 4–20 relative to the dd excitations. Therefore, due to the chosen scattering condition, the dd excitations are not negligibly weak compared to the charge-transfer excitations. The possible role of the $4p$ in the creation of valence excitations was indicated earlier.[17] In the following section, we give a general treatment of the excitations due to $3d$-$4p$ Coulomb scattering.

III. THEORY

The RIXS cross section is well described by the Kramers-Heisenberg formula,

$$I(\omega,\omega') = \sum_f |A(\omega,\mathbf{e}',\mathbf{e})|^2 \delta(\hbar\omega' + E_f - \hbar\omega), \quad (1)$$

where

$$A(\omega,\mathbf{e}',\mathbf{e}) = \langle f|D' \frac{1}{\hbar\omega - H + i\Gamma} D|g\rangle \quad (2)$$

is the scattering amplitude where $|g\rangle$ and $|f\rangle$ are the ground and final states, respectively; $D \sim \mathbf{e} \cdot \mathbf{r}$ is the electric dipole operator with $\mathbf{e}$ the polarization vector; H is the Hamiltonian of the system; and Γ is the intermediate-state lifetime broadening. We set the ground-state energy $E_g = 0$. Although we also evaluate the cross section numerically using the above expression, a better understanding of the excitations created in the process is obtained by considering the relevant terms in the scattering amplitude. We are interested in the inelastic-scattering terms arising from the indirect RIXS process[1] related to the $3d$-$4p$ Coulomb interaction contained in H'. For indirect RIXS we can expand the scattering amplitude, which gives

$$A(\omega,\mathbf{e}',\mathbf{e}) = \langle f|D' \frac{1}{\hbar\omega - \hbar\omega' - H_0 + i\Gamma} H' \frac{1}{\hbar\omega - H + i\Gamma} D|g\rangle,$$

where $H_0 = H - H'$. We want to focus on excitation to lowest order, which necessitates some approximations. We can neglect all other intermediate-state effects and treat the scattering to lowest order. This leads to the following result in lowest-order perturbation:

$$A(\omega,\mathbf{e}',\mathbf{e}) = \frac{1}{(\hbar\omega - \hbar\omega' - E_f + i\Gamma)(\hbar\omega + i\Gamma)} \langle f|D'H'D|g\rangle.$$

However, in general, intermediate-state interactions are not small, and we need to treat the intermediate-state Hamiltonian with more care. An alternative approach to the scattering amplitude is the use of the ultrashort core-hole lifetime expansion.[14] Let us express the second Green's function in terms of $|n\rangle$, which are eigenstates of H_0:

$$\sum_{nn'} |n'\rangle\langle n'| \frac{1}{\hbar\omega - E_n - H' + i\Gamma} |n\rangle\langle n|D|g\rangle. \quad (3)$$

Generally, the intermediate-state lifetime broadening Γ is a large quantity, for example, of the order of a few electron volts for transition-metal K edges. Therefore, the fine structure due to H' is smaller than Γ. In this limit, we can neglect the effect of H' in the denominator and only consider the coupling in the numerator. This gives, for the scattering amplitude,

$$A(\omega,\mathbf{e}',\mathbf{e}) = \sum_n \frac{1}{(\hbar\omega - \hbar\omega' - E_f + i\Gamma)}$$

$$\times \frac{1}{(\hbar\omega - E_n + i\Gamma)} \langle f|D'|n\rangle\langle n|H'|n\rangle\langle n|D|g\rangle.$$

The physical interpretation of this approximation at the transition-metal K edge is as follows: In the dipolar region, transitions are made into the wide $4p$ band, creating intermediate states with an energy $E_n = E_{1s} + E_{4p,m\mathbf{k}}$, where E_{1s} is the energy needed to create a deep-lying $1s$ core hole and $E_{4p,m\mathbf{k}}$ is the energy of an electron in the $4p$ band with momentum $\mathbf{k}$ and band index m. The $4p$ bandwidth is generally larger than the broadening Γ. However, the scattering between the intermediate states caused by H' is smaller than the broadening Γ. Since the effect of H' is already taken into account in the numerator, we neglect the higher-order effect in the denominator. In the emission process, the excited $4p$ electron decays and we are left with a dd excitation.

In both cases, the scattering amplitude can be split into $A(\omega,\mathbf{e}',\mathbf{e}) \cong \sum_n P_n(\omega,\omega') T_n(\mathbf{e}',\mathbf{e})$, where $P(\omega,\omega')$ is a scattering amplitude. The transitions are contained in $T_n(\mathbf{e}',\mathbf{e}) = \langle f|D|n\rangle\langle n|H'|n\rangle\langle n|D|g\rangle$, where the interaction H' is the term in the Hamiltonian responsible for creating the final-state excitations, which in our case is the Coulomb interaction between the excited $4p$ electron and the $3d$ shell. For an atom, H' can be written as[12,18]

$$H' = \sum_{\substack{kmm'qq' \\ \sigma_1\sigma_2\sigma_3\sigma_4}} \delta_{m'+q,m+q'} [c^k(dm,dm')c^k(pq',pq)F^k \delta_{\sigma_1\sigma_4}\delta_{\sigma_2\sigma_3}$$

$$- c^k(pq',dm')c^k(dm,pq)G^k \delta_{\sigma_1\sigma_3}\delta_{\sigma_2\sigma_4}]$$

$$\times p^\dagger_{q'\sigma_4}\underline{d}^\dagger_{m'\sigma_3}\underline{d}_{m\sigma_2}p_{q\sigma_1},$$

where the angular moments are $p = 1$ and $d = 2$ (for clarity, symbols are used); $p^\dagger_{q\sigma}$ creates a $4p$ electron with orbital moment q and spin σ. For late transition-metal compounds, it is more convenient to look at the scattering of holes and $\underline{d}^\dagger_{m\sigma}$ creates a $3d$ hole with orbital moment m and spin σ. F^k and G^k are the radial matrix elements of the Coulomb interaction. The coefficients c^k arise from the integrations over the angular part of the wave function and are related to Clebsch-Gordan coefficients ($3j$ symbols). In the Coulomb interaction for an atom, angular momentum is exchanged between the electrons. The first term on the right-hand side represents the direct

scattering of a p and a d electron from angular momentum q and m' to q' and m, respectively (or from m to m' for the d hole). The second term is the exchange interaction, where the p and d electrons are interchanged. At the K edge, the angular momentum of the $4p$ electron is directly related to the polarization of the x rays via the dipole operator $D \sim \sum_{q\sigma} e_q p_{q\sigma}^\dagger s_\sigma$, where s_σ creates a hole in the $1s$ core level. The components e_q of the unit polarization vector $\mathbf{e}$ can be expressed in (normalized) spherical harmonics in the direction of the polarization vector $e_q = C_{1q}(\mathbf{e}) = \sqrt{4\pi/3}Y_{1q}(\mathbf{e})$. Due to the small Coulomb exchange interaction of the $1s$ core hole with the valence shell, the $1s$ spin is unlikely to change in the intermediate state. This also implies that the spin of the $4p$ electron cannot change in the scattering process, otherwise the dipole transition for the emission is no longer allowed. For our physical understanding, it is convenient to separate the scattering of the d and p electrons. The exchange term of the p-d Coulomb interaction can be recoupled,[19] making it appear as a direct Coulomb interaction, giving for the transition operator

$$T_n = \sum_{k=0}^{2} \sum_{mm'qq'\sigma} \left(2F^k - \sum_{k'=1,3} b_{kk'}G^{k'}\right)\delta_{m'-m,q'-q}$$
$$\times c^k(1q',1q)d_{n,qq'}C_{1q'}(\mathbf{e}')C_{1q}(\mathbf{e})c^k(dm,dm')\underline{d}_{m'\sigma}^\dagger \underline{d}_{m\sigma}, \tag{4}$$

with the coefficient

$$b_{kk'} = \frac{(2k+1)n_{pk'd}^2}{n_{pkp}n_{dkd}} \begin{Bmatrix} p & k' & p \\ d & k & d \end{Bmatrix}, \tag{5}$$

where the bracketed term is a $6j$ symbol and the normalization constant

$$n_{xyz} \equiv \begin{pmatrix} x & y & z \\ 0 & 0 & 0 \end{pmatrix} \tag{6}$$

is expressed as a $3j$ symbol. Since the ground and final states do not contain $4p$ electrons and $1s$ holes, the related operators can be removed from the expression in Eq. (4). The factor 2 in front of F^k derives from the fact that the spin of the excited $4p$ electron is irrelevant for direct scattering, whereas for the exchange term the spins of the scattered d and p electrons have to be equal. The effects of the $4p$ band are given in $d_{n,qq'} = |\langle n|p_{q\sigma}^\dagger|g\rangle|^2$, which is essentially the absorption strength for a particular $4p$ orbital. Let us now assume that $d_{n,qq'} = d_n$, that is, the only polarization dependence comes from the polarization vectors and not from the details in the band structure. This condition is often well satisfied in the broad $4p$ bands. We then arrive at the central result for the effective transition operator,

$$T_n(\mathbf{e}',\mathbf{e}) = \sum_{k=0}^{2} \sum_{\kappa=-k}^{k} d_n A_k \bar{U}_\kappa^k(\mathbf{e}',\mathbf{e})W_\kappa^k, \tag{7}$$

which consists of three distinct factors. The strength of the coupling

$$A_k = (2F^k - b_{k1}G^1 - b_{k3}G^3)n_{pk}n_{dk} \tag{8}$$

with

$$n_{lx} \equiv \begin{pmatrix} l & x & l \\ -l & 0 & l \end{pmatrix} \tag{9}$$

can be expressed in terms of the radial matrix elements of the p-d Coulomb interaction as

$$A_0 = 2F^0 - \tfrac{2}{15}G^1 - \tfrac{3}{35}G^3, \tag{10}$$

$$A_1 = \tfrac{1}{5}G^1 + \tfrac{3}{35}G^3, \tag{11}$$

$$A_2 = \tfrac{4}{35}F^2 - \tfrac{1}{15}G^1 - \tfrac{3}{245}G^3. \tag{12}$$

The scattering in the valence shell is given in spherical coordinates in terms of a $3j$ symbol,[19]

$$w_q^k = \sum_{mm'q} w_{mm'q}^k \underline{d}_{m'\sigma}^\dagger \underline{d}_{m\sigma}, \tag{13}$$

where k is the rank of the scattering operator where $q = k, k-1, \ldots, -k$ are the components. The coefficients are given by

$$w_{mm'q}^k = (-1)^{d-m'} \begin{pmatrix} d & k & d \\ -m' & q & m \end{pmatrix} n_{dk}^{-1}. \tag{14}$$

The coefficients $w_{mm'\sigma}^k$ form a 5×5 matrix $w_{mm'\sigma}^k$. When considering $3d$ electrons, it is more convenient to deal with real orbitals. We can perform a unitary transformation[20,21]

$$W_\kappa^k = \sum_{q\mu\mu'\sigma} W_{\mu\mu'\kappa}^k \underline{d}_{\mu'\sigma}^\dagger \underline{d}_{\mu\sigma}, \tag{15}$$

where $W_{\mu\mu'\kappa}^k$ are the coefficients of the matrix

$$W_\kappa^k = i^k \sum_q (Z_{\kappa q}^k)^\dagger (Z^2)^\dagger w_q^k Z^2, \tag{16}$$

where

$$Z^2 = \begin{pmatrix} \frac{1}{\sqrt{2}} & 0 & 0 & 0 & -\frac{i}{\sqrt{2}} \\ 0 & -\frac{1}{\sqrt{2}} & 0 & \frac{i}{\sqrt{2}} & 0 \\ 0 & 0 & 1 & 0 & 0 \\ 0 & \frac{1}{\sqrt{2}} & 0 & \frac{i}{\sqrt{2}} & 0 \\ \frac{1}{\sqrt{2}} & 0 & 0 & 0 & \frac{i}{\sqrt{2}} \end{pmatrix} \begin{matrix} |2\rangle \\ |1\rangle \\ |0\rangle \\ |-1\rangle \\ |-2\rangle \end{matrix} \tag{17}$$

is a unitary transformation from atomic to tesseral (real) orbitals; note that $\kappa = 2,1,0,-1,-2 = x^2-y^2$, $zx, 3z^2-r^2, yz, zx$. Each of the operators has a particular angular dependence $\bar{U}_\kappa^k = \text{sgn}(\kappa)U_\kappa^k$ given by the normalized tensor product $U_\kappa^k = [\mathbf{e}'^*, \mathbf{e}]_\kappa^k$ with

$$U_0^0(\mathbf{e}',\mathbf{e}) = \mathbf{e}'^* \cdot \mathbf{e} \tag{18}$$

and

$$U_\kappa^1(\mathbf{e}',\mathbf{e}) = (\mathbf{e}'^* \times \mathbf{e})_\kappa \tag{19}$$

with $\kappa = 1,0,-1 = x,z,y$, and

$$U_2^2(\mathbf{e}',\mathbf{e}) = \sqrt{3}(e_x'^* e_x - e_y'^* e_y), \tag{20}$$

$$U_1^2(\mathbf{e}',\mathbf{e}) = \sqrt{3}(e_z'^* e_x + e_x'^* e_z), \tag{21}$$

$$U_0^2(\mathbf{e}',\mathbf{e}) = 2e_z'^* e_z - e_x'^* e_x - e_y'^* e_y, \tag{22}$$

$$U_{-1}^2(\mathbf{e'},\mathbf{e}) = \sqrt{3}(e_y'^* e_z + e_z'^* e_y), \tag{23}$$

$$U_{-2}^2(\mathbf{e'},\mathbf{e}) = \sqrt{3}(e_x'^* e_y + e_y'^* e_x). \tag{24}$$

There is a remarkable similarity between the effective transition operator in Eq. (7) and those in RIXS at the transition-metal L or M edges.[22] Within the fast-collision approximation, the RIXS scattering operator at a particular edge can be expressed in terms of spin-dependent and spin-independent operators. The latter are, apart from a constant factor, given by T in Eq. (7), but with $d_n A_k \equiv 1$. The spin-dependent operators are due to the presence of the core-hole spin-orbit coupling and are not present for the scattering due to the $4p$-$3d$ Coulomb interaction.

IV. *dd* TRANSITIONS IN NiO AND NiCl$_2$

The simplest transition operator is due to the monopole part of the p-d Coulomb interaction given by $k = 0$ and related to the F^0 radial matrix element. The effective operator is the number of holes $W_0^0 = n_h$. Since the symmetry does not change, it will not produce local dd excitations in NiO. However, it can give rise to charge-transfer type excitations of the same symmetry, although these are significantly smaller than the charge-transfer excitations due to the $1s$ core hole. For $k = 0$, the polarization part in Eq. (4) is given by the inner product $\bar{U}_\kappa^k(\mathbf{e'},\mathbf{e}) = \mathbf{e'}^* \cdot \mathbf{e}$. In a typical 90° horizontal scattering condition, this term is always zero, and we effectively "switch off" the monopole part of the p-d Coulomb interaction.

Of more interest are local dd transitions resulting from the angular momentum exchange between the $4p$ electron and the $3d$ valence band. For NiO, the ground state is $|^3A_2\rangle = |\underline{d}_{x^2-y^2\uparrow}\underline{d}_{3z^2-r^2\uparrow}\rangle$. This state $|^3A_2\rangle = |2\uparrow 0\uparrow\rangle$ in terms of tesseral harmonics. The operators W_κ^k directly couple the ground state to final state multiplets via $\underline{d}_{e_g} \rightarrow \underline{d}_{t_{2g}}$ transitions. For example, by evaluating the coefficients of the matrix in Eq. (15), we find, leaving out the spin part,

$$W_1^1|20\rangle = -\frac{1}{2}|0,-1\rangle + \frac{\sqrt{3}}{2}|2,-1\rangle, \tag{25}$$

$$W_0^1|20\rangle = |0,-2\rangle, \tag{26}$$

$$W_{-1}^1|20\rangle = -\frac{1}{2}|01\rangle - \frac{\sqrt{3}}{2}|21\rangle, \tag{27}$$

taking care of the commutation of the electrons. The quantum numbers are ordered such that the e_g holes ($\mu = 2,0 = x^2 - y^2, 3z^2 - r^2$) are in front of the t_{2g} holes ($\mu = 1,-1,-2 = zx,yz,xy$). The symmetry of this state is not directly obvious. We can, however, rewrite

$$-\frac{1}{2}|0\rangle + \frac{\sqrt{3}}{2}|2\rangle = |3x^2 - r^2\rangle, \tag{28}$$

$$-\frac{1}{2}|0\rangle + \frac{\sqrt{3}}{2}|2\rangle = |3y^2 - r^2\rangle. \tag{29}$$

We can, therefore, also write the transitions as

$$W_1^1|20\rangle = |3x^2 - r^2; yz\rangle = |T_2 - 1\rangle, \tag{30}$$

$$W_0^1|20\rangle = |3z^2 - r^2; xy\rangle = |T_2 - 2\rangle, \tag{31}$$

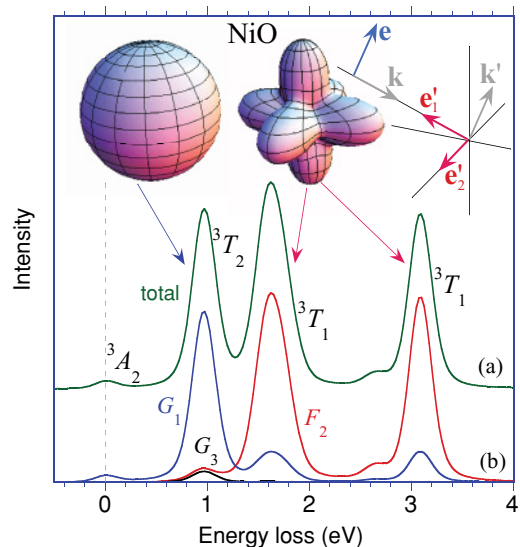$$W_{-1}^1|20\rangle = |3y^2 - r^2; zx\rangle = |T_2 1\rangle. \tag{32}$$

FIG. 2. (Color online) (a) The total RIXS intensity due to the p-d Coulomb interaction between the excited $4p$ electron and the $3d$ valence electrons in the intermediate state. A 90° horizontal scattering condition with the incoming polarization vectors 45° with respect to the z axis is used; see inset. (b) The RIXS intensity, but now separated into different terms in the p-d Coulomb interaction, where F^2 is related to the direct interaction and G^1 and G^3 are exchange interactions. The top shows the angular distributions as a function of the direction of the incoming polarization vector.

The group of $3r_i^2 - r^2$ orbitals with $r_i = x,y,z$ are invariant under symmetry operations of the octahedral group. Therefore, the symmetry of the product wave functions is equivalent to that of the t_{2g} orbitals and the total symmetry is therefore T_2. Performing the same analysis for the transitions from W_κ^2, we can write

$$|^3T_2\kappa\rangle = W_\kappa^1|^3A_2\rangle \quad \text{for} \quad \kappa = -2, -1, 1, \tag{33}$$

$$|^3T_1\kappa\rangle = W_\kappa^2|^3A_2\rangle \quad \text{for} \quad \kappa = -1, 0, 1. \tag{34}$$

W_κ^1 and W_κ^2 also lead to $\underline{d}_{e_g} \rightarrow \underline{d}_{e_g}$ transitions, which are small due to spin conservation, and $\underline{d}_{t_{2g}} \rightarrow \underline{d}_{t_{2g}}$ transitions that can be neglected due to the small t_{2g} hole density in the ground state, respectively. Figure 2(a) gives a numerical calculation of the dd transitions for a NiO$_6$ cluster[16] where the $3d$-$4p$ Coulomb interaction has been included explicitly. The F^2 Coulomb term is directly related to the W^2 operator and results predominantly in $^3T_1$ spectral weight [see Fig. 2(a)]. Some small spectral weight is present in the $^3T_1$ due to higher-order effects and other intermediate-state interactions. As a result of the recoupling, the G^1 term in the Coulomb interaction connects to the transition operators for $k = 0,1,2$. However, as can be seen from the coefficients A_k, the dominant scattering is related to the $k = 1$ term. For the $^3T_1$, the transition intensity due to G^1 is weaker relative to the F^2 by a factor of $(12F^2/7G^1)^2 \cong 5$, for a typical ratio $G^1/F^2 = 0.75$. The scattering due to the G^3 term is small. The total spectrum in Fig. 2(a) reproduces the relatively weak spectral weight of the $^3T_2$ feature with respect to the $^3T_1$ peaks. Since the $4p$-$3d$ Coulomb interaction is relatively weak, these dd can generally not be easily distinguished from the much stronger charge-transfer excitations due to the $1s$ core hole.

However, in a horizontal 90° scattering geometry (see the inset in Fig. 2), the latter excitations are strongly reduced. For a single NiO_6 unit, they would be symmetry forbidden. For a solid, these transitions become weakly allowed away from the high-symmetry axis in the Brillouin zone.

Since each of the components of the transition operators W_κ^k goes to a different final state, the angular dependence is approximately given by $\sum_{i,\kappa}[\bar{U}_\kappa^k(\mathbf{e}_i',\mathbf{e})]^2$, where $i = 1,2$ for the polarization vectors of the outgoing x rays. For a horizontal 90° scattering geometry, $\mathbf{U}^1 = \mathbf{e}_i'^* \times \mathbf{e} = -\mathbf{e}_2, -\mathbf{e}_1$ for $i = 1,2$, respectively. The angular dependence is then simply the norm of the polarization vectors and therefore a constant (see the inset in Fig. 2). For $k = 2$, the angular dependence is more complex, but straightforward to evaluate. The strongest intensity occurs when the incoming polarization vector is along a crystal axis (see Fig. 2).

V. CONCLUSION

We have demonstrated experimentally the existence of dd excitations in RIXS in the $1s \rightarrow 4p$ region in NiO and $NiCl_2$. The origin of these features is an indirect RIXS process[14] involving the Coulomb interaction between the excited $4p$ electron and the $3d$ valence electrons, creating a local dd multiplet while changing the properties of the $4p$ electron.

By employing a polarization condition that is sensitive to the changes in the $4p$ electron, dd excitations can be selectively probed. The observation of dd excitations with hard x rays provides unique benefits for applications in complex materials under real conditions.[23] At the transition-metal K edges, dd excitations can often be observed in the preedge region. This is a direct RIXS process, which is more straightforward to interpret.[9] The relative intensities of the direct and indirect RIXS processes are difficult to determine and require more experimental and theoretical investigation.

[1]For a review, see L. J. P Ament, M. van Veenendaal, T. P. Devereaux, J. P. Hill, and J. van den Brink, e-print arXiv:1009.3630.

[2]S. G. Chiuzbǎian, G. Ghiringhelli, C. Dallera, M. Grioni, P. Amann, X. Wang, and L. Braicovich, Phys. Rev. Lett. **95**, 197402 (2005).

[3]G. Ghiringhelli, A. Piazzalunga, C. Dallera, T. Schmitt, V. N. Strocov, J. Schlappa, L. Patthey, X. Wang, H. Berger, and M. Grioni, Phys. Rev. Lett. **102**, 027401 (2009).

[4]J. C. Fontecilla-Camps, P. Amara, C. Cavazza Y. Nicolet, and A. Volbeda, Nature (London) **460**, 814 (2009).

[5]M.-E. Pandelia, H. Ogata, and W. Lubitz, Chem. Phys. Chem. **11**, 1127 (2010).

[6]S.-L. Chen, V. Pelmenschikov, M. R. A. Blomberg, and P. E. M. Siegbahn, J. Am. Chem. Soc. **131**, 9912 (2009).

[7]S. W. Ragsdale, Crit. Rev. Biochem. Mol. Biol. **39**, 165 (2004).

[8]J. P. Hill, C. C. Kao, W. A. L. Caliebe, M. Matsubara, A. Kotani, J. L. Peng, and R. L. Greene, Phys. Rev. Lett. **80**, 4967 (1998).

[9]S. Huotari, T. Pylkkänen, G. Vankó, R. Verbeni, and G. Monaco, Phys. Rev. B **78**, 041102 (2008).

[10]J. P. Hill *et al.*, Phys. Rev. Lett. **100**, 097001 (2008).

[11]J. N. Hancock, G. Chabot-Couture, Y. Li, G. A. Petrakovskii, K. Ishii, I. Jarrige, J. Mizuki, T. P. Devereaux, and M. Greven, Phys. Rev. B **80**, 092509 (2009).

[12]J. S. Griffith, *The Theory of Transition-Metal Ions* (Cambridge University Press, Cambridge, United Kingdom, 1961).

[13]M. A. van Veenendaal and G. A. Sawatzky, Phys. Rev. Lett. **70**, 2459 (1993).

[14]J. van den Brink and M. van Veenendaal, Europhys. Lett. **73**, 121 (2006).

[15]B. C. Larson, W. Ku, J. Z. Tischler, C.-C. Lee, O. D. Restrepo, A. G. Eguiluz, P. Zschack, and K. D. Finkelstein, Phys. Rev. Lett. **99**, 026401 (2007).

[16]M. W. Haverkort, A. Tanaka, L. H. Tjeng, and G. A. Sawatzky, Phys. Rev. Lett. **99**, 257401 (2007).

[17]H. Kondo, S. Ishihara, and S. Maekawa, Phys. Rev. B **64**, 014414 (2001); T. Inami *et al.*, *ibid.* **67**, 045108 (2003).

[18]R. D. Cowan, *The Theory of Atomic Structure and Spectra* (University of California Press, Berkeley, CA, 1981).

[19]B. T. Thole, G. van der Laan, and M. Fabrizio, Phys. Rev. B **50**, 11466 (1994); B. T. Thole and G. van der Laan, *ibid.* **50**, 11474 (1994).

[20]M. van Veenendaal and M. W. Haverkort, Phys. Rev. B **77**, 224107 (2008).

[21]M. van Veenendaal (unpublished).

[22]M. van Veenendaal, Phys. Rev. Lett. **96**, 117404 (2006).

[23]X. Liu, M. Carpenter, Y. Shvydko, M. Upton, M. van Veenendaal, D. J. Bungum, G. Hillhouse, and S. P. Cramer (unpublished).